

# Track reconstruction in the emulsion-lead target of the OPERA experiment using the ESS microscope

October 24, 2018

L. Arrabito<sup>6</sup>, C. Bozza<sup>10</sup>, S. Buontempo<sup>7</sup>, L. Consiglio<sup>3</sup>, M. Cozzi<sup>3</sup>, N. D'Ambrosio<sup>5</sup>, G. De Lellis<sup>7</sup>, M. De Serio<sup>1†</sup>, F. Di Capua<sup>7</sup>, D. Di Ferdinando<sup>3</sup>, N. Di Marco<sup>5</sup>, A. Ereditato<sup>2</sup>, L. S. Esposito<sup>5</sup>, R. A. Fini<sup>1</sup>, G. Giacomelli<sup>3</sup>, M. Giorgini<sup>3</sup>, G. Grella<sup>10</sup>, M. Ieva<sup>1</sup>, J. Janicsko Csathy<sup>8</sup>, F. Juget<sup>8</sup>, I. Kreslo<sup>2</sup>, I. Laktineh<sup>6</sup>, K. Manai<sup>6</sup>, G. Mandrioli<sup>3</sup>, A. Marotta<sup>7</sup>, P. Migliozzi<sup>7</sup>, P. Monacelli<sup>5</sup>, U. Moser<sup>2</sup>, M. T. Muciaccia<sup>1</sup>, A. Pastore<sup>1</sup>, L. Patrizii<sup>3</sup>, Y. Petukhov<sup>4</sup>, C. Pistillo<sup>2</sup>, M. Pozzato<sup>3</sup>, G. Romano<sup>10</sup>, G. Rosa<sup>9</sup>, A. Russo<sup>7</sup>, N. Savvinov<sup>2</sup>, A. Schembri<sup>9</sup>, L. Scotto Lavina<sup>7</sup>, S. Simone<sup>1</sup>, M. Sioli<sup>3</sup>, C. Sirignano<sup>10</sup>, G. Sirri<sup>3</sup>, P. Strolin<sup>7</sup>, V. Tioukov<sup>7</sup> and T. Waelchli<sup>2</sup>.

1. Dipartimento di Fisica dell'Università di Bari and INFN, 70126 Bari, Italy
2. University of Bern, CH-3012 Bern, Switzerland
3. Dipartimento di Fisica dell'Università di Bologna and INFN, 40127 Bologna, Italy
4. JINR - Joint Institute for Nuclear Research, 141980 Dubna, Russia
5. Laboratori Nazionali del Gran Sasso, 67010 Assergi, L'Aquila, Italy
6. IPNL, IN2P3-CNRS and Université Claude Bernard Lyon, 69622 Villeurbanne, France
7. Dipartimento di Fisica dell'Università "Federico II" and INFN, 80125 Napoli, Italy
8. University of Neuchâtel, CH-2000 Neuchâtel, Switzerland
9. Dipartimento di Fisica dell'Università "La Sapienza" and INFN, 00185 Roma, Italy
10. Dipartimento di Fisica dell'Università di Salerno and INFN, 84084 Fisciano, Salerno, Italy

## Abstract

The OPERA experiment, designed to conclusively prove the existence of  $\nu_\mu \rightarrow \nu_\tau$  oscillations in the atmospheric sector, makes use of a massive lead-nuclear emulsion target to observe the appearance of  $\nu_\tau$ 's in the CNGS  $\nu_\mu$  beam. The location and analysis of the neutrino interactions in *quasi* real-time required the development of fast computer-controlled microscopes able to reconstruct particle tracks with sub-micron precision and high efficiency at a speed of  $\sim 20 \text{ cm}^2/\text{h}$ . This paper describes the performance in particle track reconstruction of the *European Scanning System*, a novel automatic microscope for the measurement of emulsion films developed for OPERA.

## 1 Introduction

In the last decades, several experiments using solar, atmospheric, reactor and accelerator neutrinos have provided unambiguous evidence for neutrino mixing. Strong

---

<sup>†</sup>Corresponding author. E-mail: Marilisa.Deserio@ba.infn.it

indications in favour of the hypothesis of  $\nu_\mu \rightarrow \nu_\tau$  oscillations in the atmospheric sector have been obtained by [1, 2, 3, 4] and have been more recently confirmed by [5, 6]. However, the direct observation of the *appearance* of oscillated  $\nu_\tau$ 's in the atmospheric  $\nu$  signal region of the parameter space is still an open issue. The OPERA experiment [7] has been designed to achieve this goal using the *CERN to Gran Sasso*  $\nu_\mu$  beam (CNGS [8]) over a baseline of 730 km.

Based on the Emulsion Cloud Chamber technique [9], nuclear emulsions [10] are used as sub-micrometric space resolution trackers to detect the  $\tau$  leptons produced in  $\nu_\tau$  charged current interactions in a massive ( $\mathcal{O}(\text{kt})$ ) lead target.

The basic target unit (*brick*) with size  $12.7 \times 10.2 \times 7.5 \text{ cm}^3$  consists of 57 nuclear emulsion films, made of two  $44 \mu\text{m}$ -thick layers on either side of a  $205 \mu\text{m}$  plastic base, interleaved with 56 lead plates of 1 mm thickness. Bricks are arranged in vertical structures called *walls*.

Electronic trackers, made of planes of plastic scintillator strips inserted in between the target walls, and muon spectrometers accomplish the task of identifying in real-time the position of the neutrino interaction inside the target. As a result of the combined analysis of electronic data, a 3-D brick probability map is computed for each single event and the brick with the highest probability is promptly removed from the target during the run. The so-called *Changeable Sheets* (CS), pairs of emulsion films placed in front of each brick and acting as interfaces with the electronic trackers, allow the brick identification signal to be checked. Only in case of confirmation, the emulsion films of the brick are developed and sent to the scanning laboratories for interaction vertex location and further analysis.

Assuming the nominal intensity of the CNGS beam ( $4.5 \times 10^{19}$  p.o.t. / year), about 30 bricks per day will be extracted from the target, corresponding to a total surface of nuclear emulsions to be scanned of a few thousands  $\text{cm}^2$  per day<sup>1</sup>. In order to analyze the events in *quasi* real-time with a reasonable number of microscopes ( $\sim 1$  microscope / brick / day), the use of fast automatic systems with a scanning speed of about  $20 \text{ cm}^2/\text{h}$  is required.

Moreover, the detection of the short-lived  $\tau$  leptons through the observation of their *kink* decay topology, namely an abrupt deviation of the  $\tau$  particle trajectory at the decay point in electron, muon and charged hadron(s), occurring over distances of  $\sim 1 \text{ mm}$  at CNGS energy, demands adequate position ( $\lesssim 1 \mu\text{m}$ ) and angular ( $\sim 1 \text{ mrad}$ ) resolutions.

The *European Scanning System* (ESS) was designed to meet these experimental requirements<sup>2</sup>. The general structure of the system and the algorithms developed for image processing and particle tracking in single emulsion films, as well as the hardware and its performance, have been already described in detail [12, 13, 14]. The performance in electron-pion separation has been recently published in [15].

In this paper, after a brief summary of the main features of the ESS, the film-by-film alignment algorithm, relevant for the analysis of OPERA bricks, and the

---

<sup>1</sup>The position resolution of the electronic trackers ( $\sim 1 \text{ cm}$ ) will allow to reduce the area to be scanned to  $\sim 25 \text{ cm}^2$  for CC interactions with penetrating muon tracks. For NC events, we foresee to scan the whole surface.

<sup>2</sup>A different system for the scanning of OPERA films at high speed has been developed in Japan (SUTS [11]).

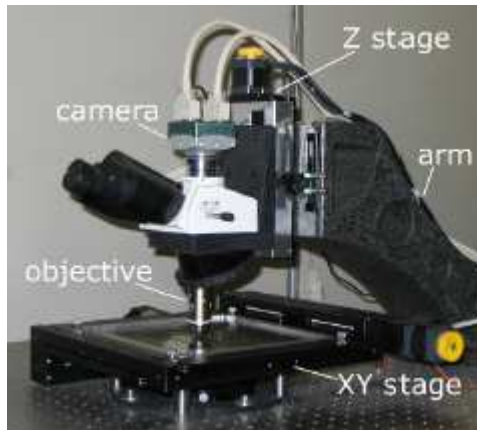


Figure 1: The *European Scanning System* microscope.

tracking performance of the system are presented. The methods to be applied for the location of neutrino events are then described and the results of a beam exposure to high-energy pions, designed to test the above procedures, are reported.

## 2 The European Scanning System

The ESS microscope, shown in Fig. 1, consists of

- computer driven horizontal and vertical stages equipped with high-speed precision mechanics;
- customized optics providing achromatic planar images of the emulsion;
- high resolution and high frame-rate camera interfaced with a programmable frame-grabber and vision processor.

By adjusting the focal plane of the objective lens through the whole emulsion thickness, a sequence of tomographic images of each field of view are taken at equally spaced depth levels, processed and analysed in order to recognise aligned clusters of dark pixels (*grains*) produced by charged particles along their trajectories. Each  $44\ \mu\text{m}$ -thick OPERA emulsion layer is spanned by 15 tomographic images in steps of  $\sim 3\ \mu\text{m}$ , accounting for the effective focal depth of the system.

*Micro-tracks* are reconstructed as geometrical alignments of grains detected in different levels within the same layer. By connecting micro-tracks across the plastic support, the so-called *base-tracks* are formed (Fig. 2). This strongly reduces the instrumental background due to fake combinatorial alignments, thus significantly improving the signal to noise ratio, and increases the precision of track angle reconstruction by minimising distortion effects.

The reconstruction of particle tracks in OPERA bricks requires connecting base-tracks in several consecutive films.

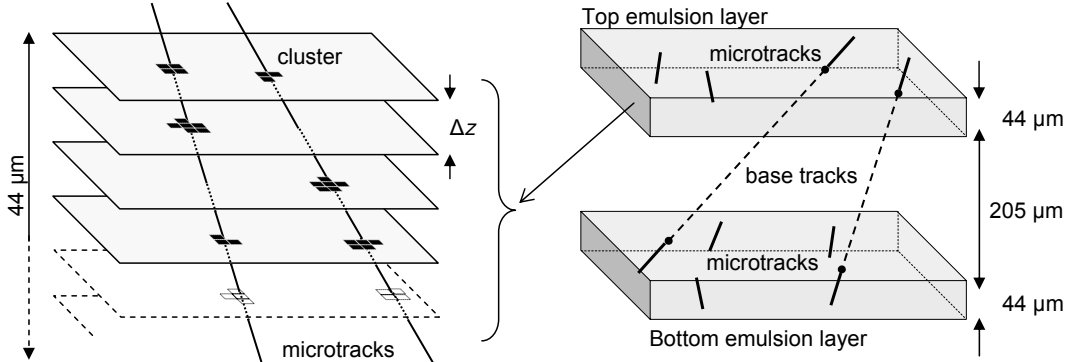


Figure 2: Micro-track connection across the plastic base (base-track).

### 3 Emulsion film alignment

In order to define a global reference system (hereafter referred to as *brick* reference system), prior to track reconstruction a set affine transformations (shift, rotation and expansion) relating track coordinates in consecutive films have to be computed to account for relative misalignments and deformations. The mechanical accuracy of film piling in brick assembly is indeed of  $50 \div 100 \mu\text{m}$ , much worse than the achievable precision. Furthermore, emulsion films are affected by environmental conditions (temperature and humidity) altering their original geometry. The task of film alignment is accomplished by exposing each brick to a controlled flux of cosmic rays before disassembly, as described in [16], and by applying the following procedure film by film.

Starting from a set of independent measurements in single emulsion films, an aligned volume is created through an iterative pattern matching procedure computing the parameters of the transformations

$$\begin{pmatrix} x^{brick} \\ y^{brick} \end{pmatrix} = \begin{pmatrix} a_{11} & a_{12} \\ a_{21} & a_{22} \end{pmatrix} \begin{pmatrix} x^{film} \\ y^{film} \end{pmatrix} + \begin{pmatrix} b_1 \\ b_2 \end{pmatrix},$$

where  $x^{film}$ ,  $y^{film}$  are single film track coordinates and  $x^{brick}$ ,  $y^{brick}$  are the corresponding *aligned* ones. A least square fit is applied after maximising the number of matching pairs within predefined position and slope tolerances measured in three zones, typically chosen at the corners of the scanned area in order to maximise the lever arm and thus disentangle the contributions due to rotation and translation.

Moreover, a wide angular spectrum of collected tracks allows the total thickness of the emulsions and of the interleaved lead plates to be precisely computed, accounting for possible a-planarities. The difference between the real position of a given track in the  $i$ -th film and the extrapolated position from the  $j$ -th film depends indeed on the uncertainty  $\delta Z$  on the knowledge of the thickness and is a linear function of the track angle. By using a set of tracks crossing the brick at different inclination angles, a fit can be performed and the correction to be applied to

the nominal value of the Z coordinate, perpendicular to the emulsion plane, can be estimated, thus improving the quality of the alignment.

By applying the above procedure to each pair of consecutive films, relative displacements can be reduced to the level of a few  $\mu\text{m}$ , adequate for film-by-film track following (see Section 5), down to less than  $1\ \mu\text{m}$ , as required by local-scale ( $\sim 1\ \text{mm}$ ) analysis (this subject will be discussed in forthcoming papers).

The achievable precision mainly depends on the number of penetrating tracks, proportional to the area of the measured zones. The density of passing-through tracks should be low enough in order not to spoil the topological and kinematical reconstruction of neutrino events; on the other hand, the scanning time is a critical issue and needs to be minimised. Typically, a density of the order of a few tracks  $/\text{mm}^2$  and scanning zones of  $\mathcal{O}(10\ \text{mm}^2)$  are a reasonable compromise between these two conflicting requirements.

Once all films have been aligned, base-tracks are connected to form *volume tracks*. A two-step algorithm is applied [17]. The first step consists of identifying incremental *chains* of consecutive base-tracks. These chains are then used as input for the Kalman filter algorithm [18], performing track fitting and propagation with a maximum number of allowed consecutive *holes* (i.e. missing segments) accounting for tracking inefficiency.

## 4 Study of the ESS basic performance

In order to study the track reconstruction performance of the ESS in terms of resolution and efficiency, a test exposure was performed at the CERN PS in the T7 experimental area. One brick consisting of 64 emulsion films with no lead plates in between was exposed to  $10\ \text{GeV}/c$  negatively-charged pions. The choice of high beam momentum and the use of emulsions only were motivated by the need to minimise the effect of multiple Coulomb scattering that would spoil the measurement of the intrinsic resolution.

The emulsion films, produced by the Fuji Film<sup>3</sup> company, were similar to those used for the experiment, although they were not part of the official OPERA production. They were transported by plane from Japan to CERN where the *refreshing* procedure was applied shortly before exposure.

Nuclear emulsions are continuously sensitive to charged particles from production time until development. As a consequence, they normally accumulate a significant amount of background due to cosmic rays and ambient radioactivity that cannot be distinguished from particle tracks originating from the beam. For this reason, a process of controlled fading of the emulsions, called *refreshing*, consisting in the destruction of latent image centers in silver bromide crystals by keeping the films at high temperature and high relative humidity for a few days, was implemented for the OPERA experiment [19]. The working conditions can be tuned in order to reduce the average number of grains per base-track below the applied threshold, while preserving the emulsion sensitivity. This implies the *cancellation* of recorded tracks. The achieved track erasing efficiency can be higher than 98%.

---

<sup>3</sup>Fuji Film, Minamiashigara, 250-0193, Japan.

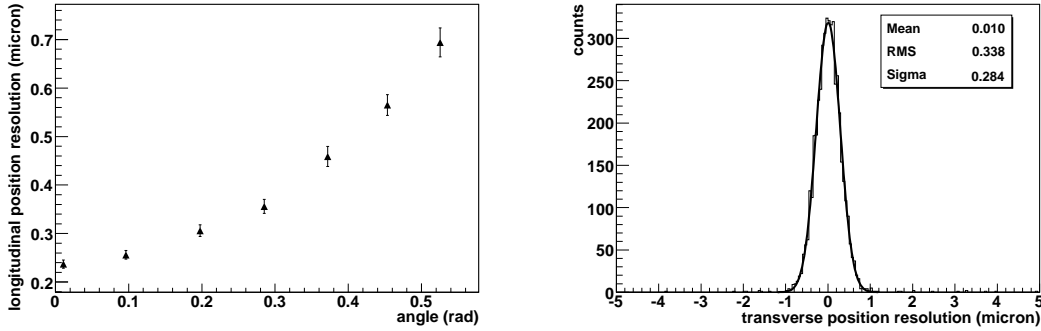


Figure 3: Longitudinal position residuals between base-tracks and corresponding volume tracks as a function of track angle (left); transverse position residuals (right).

The angular dependence of the ESS tracking efficiency and precision were studied by rotating the brick with respect to the beam direction in 7 different positions from 0 mrad (tracks perpendicular to the films) to 600 mrad. The pion beam and the exposure time were adjusted so as to produce a density in emulsion of about 3 tracks /mm<sup>2</sup> for each angle. Reference emulsions not exposed to the pion beam were also developed to provide an evaluation of the instrumental background, mainly due to uncorrelated grains randomly produced in the development process (*fog*) that tend to hide real track grains, hence resulting in fake coincidences.

In order to collect a sample of several hundred tracks per angle exposure, an area of a few cm<sup>2</sup> was scanned for each film and a pattern-matching procedure was applied to compute the parameters of film inter-calibration transformations, as described in Section 3. Measured base-tracks were then connected to form volume tracks.

Fig. 3 shows the position residuals between each base-track and the corresponding fitted volume track as a function of the track angle. If  $\mathbf{S} = (s_x, s_y)$  is the slope vector of a straight line representing the projection of a particle track in the horizontal plane, the unit vectors  $\mathbf{n}_{\parallel} = (n_x, n_y)$  such that  $\mathbf{S} = S \mathbf{n}_{\parallel}$  and its normal  $\mathbf{n}_{\perp} = (n_y, -n_x)$  define two orthogonal directions, called *longitudinal* and *transverse*, that can be used to decouple the slope-dependent contribution from the intrinsic accuracy. The longitudinal component is indeed affected by a slope-dependent term proportional to the uncertainty on the Z positions of grains that can be assumed to be given by the sampling step of the tomographic sequence [12].

The left plot of Fig. 3 shows longitudinal residuals ranging from 0.3  $\mu\text{m}$  to 0.7  $\mu\text{m}$ . Transverse residuals (right plot) are independent of track angle and represent the ultimate precision (0.3  $\mu\text{m}$ ) that can be achieved accounting for measurement errors.

The angular residuals, computed as differences between base-track and volume-track angles, are shown in Fig. 4. Perpendicular tracks (left) can be reconstructed with a resolution of about 1.7 mrad; the resolution worsens with the angle up to 6.3 mrad for tracks crossing the brick at about 600 mrad with respect to the perpendicular direction (right).

In order to evaluate the tracking efficiency, minimizing the effect of base-tracks

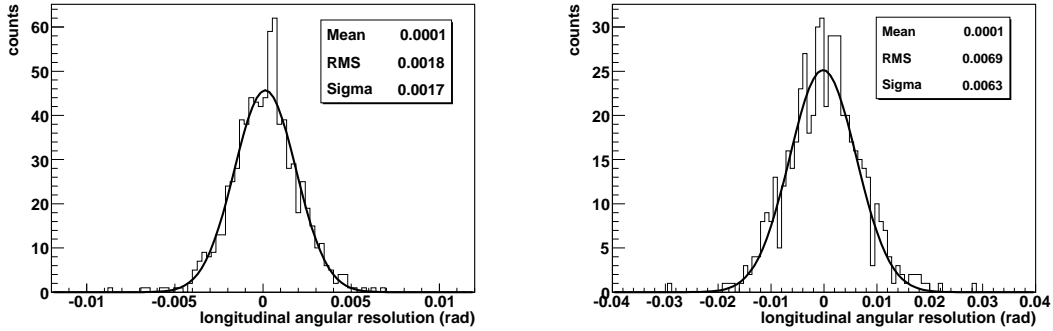


Figure 4: Angular residuals between base-tracks and corresponding volume tracks for particles crossing the emulsions perpendicularly (left) and at 600 mrad inclination (right).

not related to the beam, sets of six adjacent films were aligned and beam volume-tracks<sup>4</sup> with at least five consecutive base-track segments were selected. Set by set, the efficiency was computed for the two external films as the ratio between the number of tracks with six measured segments and the number of tracks with five measured base-tracks only. By averaging over several films, the plot in Fig. 5 was obtained. The base-track finding efficiency is larger than 90% for perpendicular tracks; correspondingly, the micro-tracking efficiency, as given by its square root<sup>5</sup>, is above 95%.

The shape of the curve in Fig. 5 is related to the slope dependence of the average number of grains per base-track shown in Fig. 6: for small angles, the *shadowing* effect (see [12]) enhances the signal, thus improving the efficiency. The effect falls off with increasing slope. However, for sufficiently large angles, the increase in the average number of grains due to longer path length in emulsion produces again an increase of the efficiency.

The background measurement was performed using unexposed reference films refreshed and developed at the same time as the other films. A few hundred base-tracks selected applying standard cuts (see [12]) were visually inspected in order to separate the contribution due to residual cosmic rays from instrumental background, consisting of base-tracks with at least one micro-track generated by accidental combinations of fog grains. About 1 fake base-track /cm<sup>2</sup> was found in the angular range [0, 400] mrad.

The measurements presented in this section were performed with the ESS working at its maximum speed of  $\sim 20$  cm<sup>2</sup>/h.

<sup>4</sup>Beam tracks were defined as those with a reconstructed angle within  $3\sigma$  from the center of any of the 7 beam peaks.

<sup>5</sup>Micro-tracks in the two emulsion layers of each film are independently recognised and the efficiency of the linking procedure can be assumed equal to 1 since it only depends on geometrical acceptances that can be properly tuned.

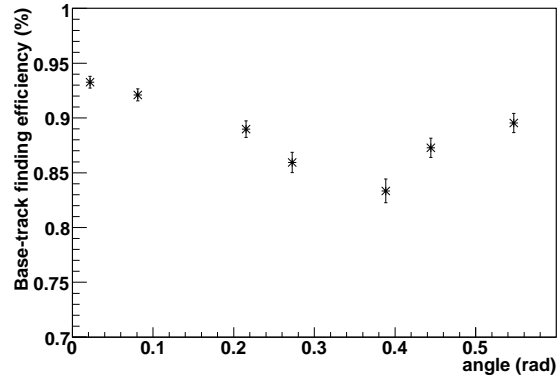


Figure 5: Base-track finding efficiency as a function of track angle.

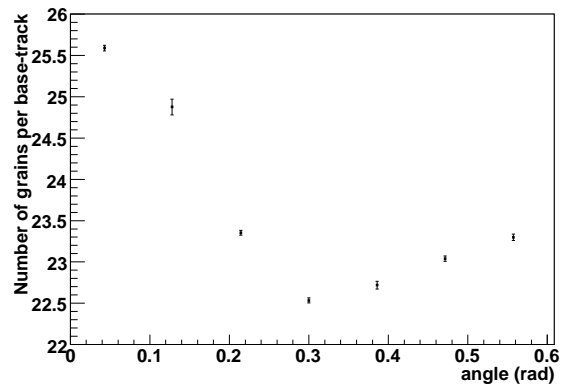


Figure 6: Average number of grains per base-track as a function of track angle.



## 5 Particle track reconstruction in OPERA bricks

Two different steps are foreseen in the event location strategy we plan to apply for the analysis of the OPERA bricks. The first procedure is the so-called *scan-back*: starting from a set of predictions provided by the electronic detectors, tracks of secondary particles coming from a neutrino interaction are searched for in the CS films; then, these tracks are followed back, film by film, from the most downstream emulsion of the brick to the interaction point where they originate. Whenever a track disappearance signal is detected (the track is not found in a certain number of consecutive films set according to the tracking efficiency), an area of about  $25\text{ mm}^2$  is measured in several films around the candidate vertex point (*volume scan*) in order to fully reconstruct the event and apply topological and kinematical selection criteria.

In order to test the system capability in reconstructing particle tracks in the OPERA emulsion-lead target, several bricks assembled with *refreshed* films were exposed to a low intensity  $8\text{ GeV}/c\ \pi^-$  beam at the CERN PS - T7 line. CS films, packed under vacuum in a separate envelope, were attached to the downstream face of each brick.

About 1000 pions with inclination angles of about  $50\text{ mrad}$  with respect to the perpendicular direction were recorded in each target unit over an area of  $9 \times 9\text{ cm}^2$ . Before unpacking and development, CS films were removed<sup>6</sup> and each brick was exposed to cosmic rays for 6 hours in order to collect a set of passing-through tracks (density  $\sim 1\text{ track}/\text{mm}^2$ ) to be used for film alignment.

The OPERA event location procedure starting from CS films was mimicked using the tracks found in both CS's and confirmed in the most downstream film of the brick as predictions. Film by film, each track was searched for in one single microscope view ( $390 \times 310\ \mu\text{m}^2$ ) within a slope-dependent angular window, accounting for the decrease in accuracy with increasing angle. In case two or more base-tracks satisfied the angular cut, the closest-distance criterion was used for selection<sup>7</sup>. Track propagation from film to film was performed by using the position and the slope of the most upstream track segment. Losses due to tracking inefficiency were recovered by requiring that the search for each track be iterated in 3 consecutive emulsion films if no candidate was found in one film. In case no base-track compatible with the prediction was found in 3 films, the position of the most upstream measured base-track was tagged as a candidate vertex point and the volume scan procedure was applied around it.

The tracking efficiency, computed as the number of found base-tracks divided by the total number of films for the sample of passing-through particles (mainly primary pions and muons from beam contamination), is shown in Fig. 7. The measured value ( $\sim 93\%$ ) is in agreement with the expected behaviour at small angle shown in Fig. 5.

---

<sup>6</sup>Since the scanning of the CS films is a crucial step in the event location procedure (only tracks measured in the CS films are followed-back across the brick), the background track density should be kept as low as possible.

<sup>7</sup>Different best-candidate selection criteria (for example, criteria based on the angular agreement) are currently being tested.

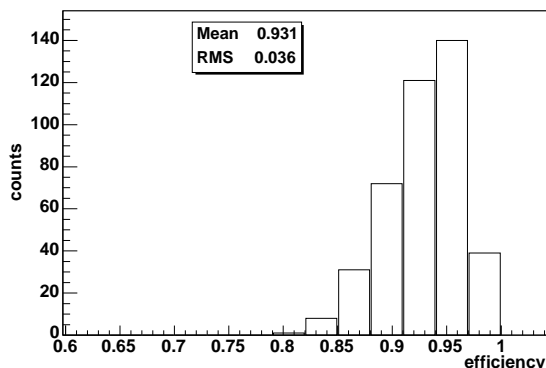


Figure 7: Tracking efficiency for non-interacting particles.

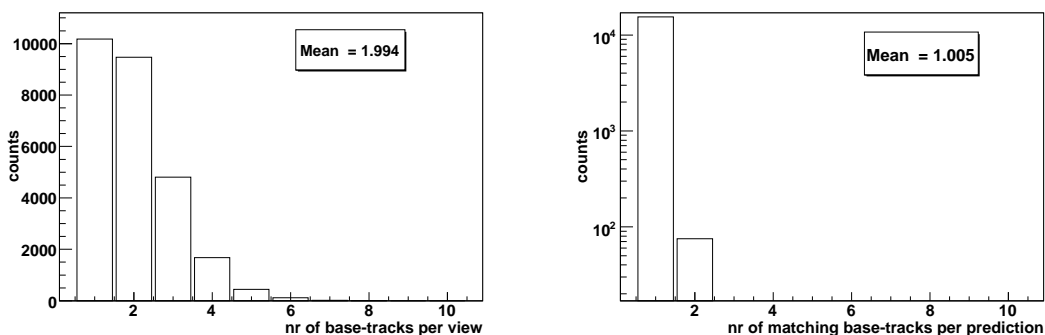


Figure 8: Left: Number of base-tracks per view. Right: Number of base-tracks per prediction satisfying the selection criteria.

On average, 2 base-tracks with space angles smaller than 400 mrad were reconstructed in each microscope view around the position of a given predicted track (Fig. 8, left). By requiring that the slope difference between found and predicted base-tracks be not larger than  $(0.03 + 0.05 \times \text{slope})$ , hence allowing for the non-negligible contribution due to the scattering of low energy particles in lead, the average number of candidates per prediction reduces to 1, the fraction of predictions with multiple candidates being of the order of  $10^{-3}$  (Fig. 8, right).

We foresee to complete the scanning of each brick in a few hours. In order to minimise the scanning time required for event location, fine corrections are not applied in scan-back mode. First of all, only a *global* film inter-calibration procedure is performed. Fig. 9 shows the distribution of the position differences between predicted and found base-track segments. The plot refers to tracks scattered over an area of about  $40 \text{ cm}^2$ . The sigma of the gaussian fit is of about  $7 \mu\text{m}$ . Moreover, only one microscope view is measured for each predicted track, thus effects such as local planarity cannot be corrected. The resulting angular precision is of about  $4 \div 5 \text{ mrad}$ .

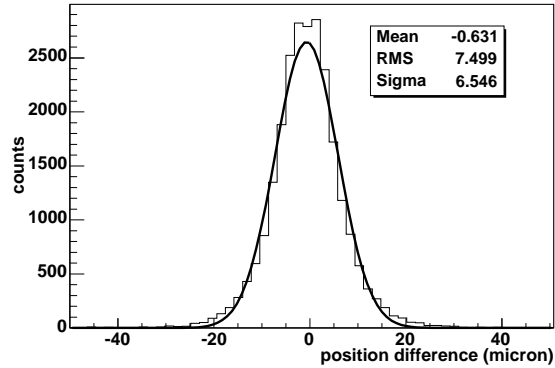


Figure 9: Position differences between predicted and found base-track segments. Tracks are distributed over an area of about  $40 \text{ cm}^2$ .

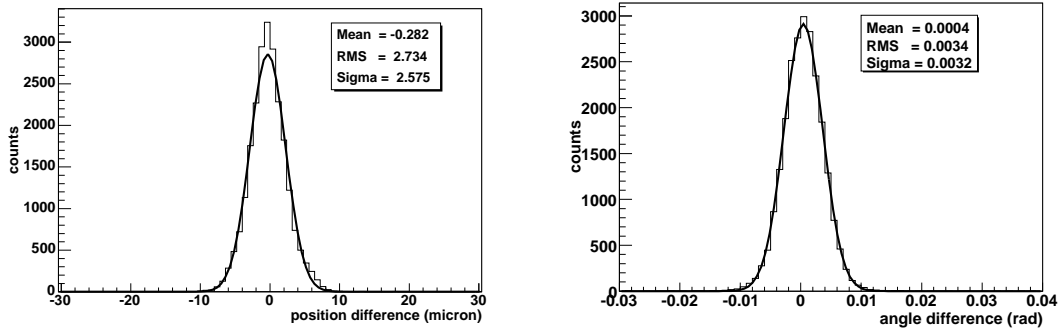


Figure 10: Position (left) and angle (right) differences between base-tracks selected in two scan-back procedures corresponding to the same set of predictions.

The scan-back reproducibility was studied by performing the procedure twice for the same set of predictions and by comparing film by film the selected base-tracks per each predicted track. As shown in Fig. 10, the reproducibility is of about  $2.6 \mu\text{m}$  in position and  $3 \text{ mrad}$  in angle.

As a cross-check for the validation of scan-back results, the volume scan procedure was applied around track disappearance points and, by a combined analysis of scan-back and volume scan data, events were classified as single and multi-prong interactions, low energy (scattering) tracks and passing-through tracks. Film-dependent effects, such as local distortion and misalignments resulting from large rotations, not completely corrected in the inter-calibration procedure, were found to be the main sources of inefficiency ( $< 5\%$ ) in the track following. Such effects can be accounted for by enlarging the search window in case no base-tracks compatible with a given prediction are found and by implementing a *prediction-forking* method, allowing for multiple candidate following, if the slope/position acceptances are increased. Failures of the system in passing-through track following can be thus

reduced to  $\sim 1\%$ .

## 6 Conclusions

The particle tracking performance of the European Scanning System (ESS), a novel high-speed automatic microscope for the measurement of nuclear emulsion films, has been presented.

The system, developed for the location and analysis of neutrino interactions in the emulsion-lead target of the OPERA experiment, fully satisfies the requirements of high tracking efficiency and accuracy, working at a speed of  $\sim 20 \text{ cm}^2/\text{h}$ .

The results of a test exposure to high-energy pions, designed to study the methods to be applied for film-by-film alignment, track following and event location and confirmation, were discussed in details, showing that the system is able to track particles produced in beam interactions with lead through the whole brick and identify the vertex points where they originate. The achieved results make us confident in view of forthcoming CNGS neutrino runs.

## Acknowledgements

We acknowledge the cooperation of the members of the OPERA Collaboration and we thank many colleagues for discussions and suggestions. We gratefully acknowledge the invaluable support of the technical staff in our laboratories; in particular, we thank A. Andriani, P. Calligola, P. Di Pinto, M. Hess, H. U. Schuetz, C. Valieri for their contributions. We acknowledge support from our funding agencies. We thank INFN for providing fellowships and grants (FAI) for non Italian citizens.

## References

- [1] Y. Fukuda, et al., Phys. Rev. Lett. 81 (1998) 1562; J. Hosaka, et al., Phys. Rev. D 74 (2006) 032002; K. Abe, et al., Phys. Rev. Lett. 97 (2006) 171801.
- [2] K. S. Hirata, et al., Phys. Lett. B 205 (1988) 416.
- [3] M. Ambrosio, et al., Phys. Lett. B 434 (1998) 451; M. Ambrosio, et al., Phys. Lett. B 566 (2003) 35; M. Ambrosio, et al., Eur. Phys. J. C 36 (2004) 323.
- [4] W. W. M. Allison, et al., Phys. Lett. B 449 (1999) 137; W. W. M. Allison, et al., Phys. Rev. D 72 (2005) 052005.
- [5] M. H. Ahn, et al., Phys. Rev. D 74 (2006) 072003.
- [6] D. G. Michael, et al., Phys. Rev. Lett. 97 (2006) 191801.
- [7] M. Guler, et al., CERN-SPSC-2000-028; R. Acquafredda, et al., New J. Phys. 8 (2006) 303.

- [8] G. Acquistapace, et al., CERN-98-02, INFN/AE-98/05 (1998); R. Bailey, et al., CERN-SL-99-034, INFN/AE-99/05 (1999); A.E. Ball, et al., SL-Note 2000-063 (2000);  
<http://proj-cnsgs.web.cern.ch/proj-cnsgs>.
- [9] M. Kaplon, B. Peters and D. Ritson, Phys. Rev. 85 (1952) 900.
- [10] W. H. Barkas, Nuclear Research Emulsion, Academic Press, London (1963); C. F. Powell, P. H. Fowler and D. H. Perkins, The study of elementary particles by the photographic method, Pergamon Press, New York (1959).
- [11] S. Aoki, et al., Nucl. Instr. Meth. B 51 (1990) 466; T. Nakano, Proceedings of the International Europhysics Conference on High Energy Physics, Budapest, Hungary, 12-18 July 2001.
- [12] N. Armenise, et al., Nucl. Instr. Meth. A 551 (2005) 261-270.
- [13] L. Arrabito, et al., Nucl. Instr. Meth. A 568 (2006) 578.
- [14] M. De Serio, et al., Nucl. Instr. Meth. A 554 (2005) 247.
- [15] L. Arrabito, et al., JINST 2 (2007) P02001.
- [16] E. Barbuto, et al., Nucl. Instr. Meth. A 525 (2004) 485.
- [17] V. Tioukov et al., Nucl. Instr. Meth. A 559 (2006) 103.
- [18] R. K. Bock and M. Regler, Data analysis techniques for high-energy physics experiments, Cambridge University Press (1990); R. Frühwirth, Nucl. Instr. Meth. Phys. Res. A 262 (1987) 444.
- [19] T. Nakamura, et al., Nucl. Instr. Meth. A 556 (2006) 80.